UCRL-JRNL-212538

LAWRENCE
LIVERMORE
NATIONAL
LABORATORY

Radiation induced crosslinking in a silica-filled silicone elastomer as investigated by multiple quantum H NMR

R. S. Maxwell, S. C. Chinn, D. Solyom, R. Cohenour

May 25, 2005

Macromolecules

Disclaimer

This document was prepared as an account of work sponsored by an agency of the United States Government. Neither the United States Government nor the University of California nor any of their employees, makes any warranty, express or implied, or assumes any legal liability or responsibility for the accuracy, completeness, or usefulness of any information, apparatus, product, or process disclosed, or represents that its use would not infringe privately owned rights. Reference herein to any specific commercial product, process, or service by trade name, trademark, manufacturer, or otherwise, does not necessarily constitute or imply its endorsement, recommendation, or favoring by the United States Government or the University of California. The views and opinions of authors expressed herein do not necessarily state or reflect those of the United States Government or the University of California, and shall not be used for advertising or product endorsement purposes.

Radiation induced crosslinking in a silica-filled silicone elastomer as investigated by multiple quantum ^{1}H NMR.

Robert S. Maxwell[1], Sarah C. Chinn[1], David Solyom[2], and Rebecca Cohenour[2]*

[1]Lawrence Livermore National Laboratory, 7000 East Ave, Livermore, CA 94551

[2]Honeywell Inc. Federal Manufacturing & Technologies, Kansas City, MO 64141

RECEIVED DATE

Running title: "MQ-NMR of Radiation damage in filled siloxanes"

CORRESPONDING AUTHOR FOOTNOTE: Mail code: L-231, (925) 423-4991, (925) 422-3750, maxwell7@llnl.gov

ABSTRACT: DC745 is a commercially available silicone elastomer consisting of dimethyl, methyl-phenyl, and vinyl-methyl siloxane monomers crosslinked with a peroxide vinyl specific curing agent. It is generally considered to age gracefully and to be resistant to chemical and thermally harsh

environments. However, little data exists on the radiation resistance of this commonly used silicone elastomer. We report static ^{1}H NMR studies of residual dipolar couplings in DC745 solid elastomers subject to exposure to ionizing gamma radiation. ^{1}H spin-echo NMR data shows that with increasing dose, the segmental dynamics decrease is consistent with radiatively induced crosslinking. ^{1}H multiple quantum NMR was used to assess changes in the network structure and observed the presence of a bimodal distribution of residual dipolar couplings, $<\Omega_d>$, that were dose dependent. The domain with the lower $<\Omega_d>$ has been assigned to the polymer network while the domain with the higher $<\Omega_d>$ has been assigned to polymer chains interacting with the inorganic filler surfaces. In samples exposed to radiation, the residual dipolar couplings in both reservoirs were observed to increase and the populations were observed to be dose dependent. The NMR results are compared to Differential Scanning Calorimetry (DSC) and a two-step solvent swelling technique. The solvent swelling data lend support to the interpretation of the NMR results and the DSC data show both a decrease in the melt temperature and the heat of fusion with cumulative dose, consistent with radiative crosslinking. In addition, DSC thermograms obtained following a 3 hr isothermal soak at -40 ºC showed the presence of a second melt feature at T_m ~ -70 ºC consistent with a network domain with significantly reduced segmental motion.

KEYWORDS: siloxanes, radiation, crosslinking, Multiple quantum NMR, polymer-filler interactions

INTRODUCTION**:** As polymeric materials are required to endure ever increasing lifetimes in service there is a fundamental need to employ sensitive and versatile *in situ* methods to investigate the structural and motional changes that occur in these materials as a result of use in chemically, thermally, or radioactively harsh environments. Ideally, these methods would allow a complete assessment of aging mechanisms in order to yield predictive capabilities. For example, it has been well recognized that time dependent changes in network structure (e.g. domain sizes, morphology, and crosslink density) can contribute to degradation in engineering performance over decades and numerous methods have been developed to assess such changes. It is, in addition, generally understood that changes in the physical and chemical interactions between reinforcing fillers and the polymer network will also contribute to the long term performance of filled elastomeric components. There are few spectroscopy techniques, however, that are generally capable of probing this regime.

Nuclear magnetic resonance (NMR) has gained much attention in the last few decades for its ability to non-destructively characterize changes in chemical composition and network structure in a broad range of polymer systems.[1-25] Static ^{1}H Multiple Quantum NMR methods which measure the residual dipolar couplings, in specific, hold much promise for such efforts.[13-20,24] In elastomeric materials, the residual dipolar couplings have been shown to be the result of topological constraints interfering with fast reorientations on the NMR timescale that otherwise would be expected to average homonuclear dipolar couplings to zero.[9] The residual dipolar couplings, in fact, have been shown to be quite sensitive to network and morphological changes and have been used to test theories of polymer structure, ordering, and dynamics. These residual dipolar couplings can be quantitatively assessed using a variety of NMR experimental protocols, including relaxation methods, ^{2}H and ^{1}H lineshape analysis, modulation of the stimulated echo, and the magic-echo which has been shown to be superior for assessing residual dipolar couplings than either the solid echo or the stimulated echo .[4-25]

More recently, it has been reported that the characterization of the growth of multiple quantum coherences can provide detailed insight into silicone network structure by increasing the selectivity of the NMR experiment to the structure and dynamics most connected to the topology of the polymer network, including chain ordering at the surface of inorganic filler particles.[13-24] In addition, it has been shown that echo based methods can over estimate the residual dipolar couplings due to the effects of magnetic susceptibilities and field gradients due to internal microscopic voids and the inorganic filler.[28] These effects have been observed to be large enough to reverse trends of $<\Omega_d>$ vs crosslink density at different fields.[29, 30] MQ based approaches, have so far, been shown to be insensitive to these effects.[30] Since the network topology and the filler-particle interactions determine to a significant part the engineering properties,[31] including tensile, shear, and creep moduli, MQ methods offer the potential for model free insight into the origins of degradation in material performance.

In this paper, we examine the effects of radiation dose on the microstructure and polymer chain mobility of DC-745, a complex, commercial, crosslinked and filled silicone elastomer using static ^{1}H echo and multiple quantum NMR methods. These methods provide insight into the changes in both the network structure and the polymer filler interface. The data is interpreted in combination with solvent swelling and DSC studies. Though there has been significant application of NMR to silicone based polymeric materials [see, for example, references 4-9,17-19, 22-23], no systematic study of the effects of radiation on DC745 nor the application of these multiple quantum methods to radiation induced damage at the filler-polymer interface in silicones have been reported previously.

EXPERIMENTAL: Samples were cured from Dow Corning 745U silicone fluid with 2,5-Dimethyl-2,5-di(t-butylperoxy)hexane peroxide curing agent supported on $CaCO_3$ (Dow Corning). DC745U fluid is a proprietary mixture of monomer composition. ^{1}H and ^{29}Si{^{1}H} NMR has determined that the elastomers studied here contained ~ 98.5% dimethyl siloxane monomers, ~ 1.5% methyl-phenyl siloxane

monomers, and a small amount of vinyl siloxane monomers that are converted to short chain (presumably N=4) alkyl crosslinking junctions. Curing was performed by thermal activation at 170 °C for 10 minutes. The final elastomer also contains ~30 wt.% mixture of quartz and high surface area fumed silica fillers and small amounts of $CaCO_3$ remaining from the curing agent for thixotropic thickening and tear resistance. The fully cured composites were sealed in glass ampoules evacuated and backfilled with N_2. The ampoules were then placed in a 1 L stainless steel canister and lowered into the irradiation pit. The irradiation pit contained a Co-60 source (1.2 MeV). The samples were irradiated at 5 kGray/hr for times necessary to expose the samples to 30 kGray to 250 kGray.

DSC analyses were performed (TA Instruments, MDSC Q1000, New Castle, DE) by cooling the sample at a rate of 30°C/min. to –150 °C from room temperature. Subsequent heating of the samples was then performed at 3 °C/min. with a modulation frequency of ±0.40°C/50 sec. The pristine copolymer was characterized by a crystallization temperature @ -45 ºC and a glass transition temperature @ -120 ºC. A second set of analyses were then performed that included a 3 hr isothermal soak at -40 ºC on the cool down cycle.

Details of the two-step solvent swelling based on the method developed by Polmanteer and Lentz have been described elsewhere.[6-8, 32-34] The samples (~1 g) were first weighed for the initial dry weight and then submerged in 600 ml of toluene (Aldrich, Milwaukee, WI) in a sealed Teflon container while stirring. Periodically, the swollen weight of the sample was measured until an equilibrium weight was obtained (~ 3 days). Once saturation equilibrium had been established, 150 ml of concentrated ammonia (28 wt.%, Aldrich, Milwaukee, WI)) was added directly to the toluene solution, the container was resealed, and stirring continued. The ammonia effectively severs the hydrogen bonding interaction between the surface silanols on the filler and the siloxane backbone of the polymer. The ammonia is of limited solubility in toluene and it is expected that only a fraction of the ammonia enters the polymer-toluene phase and that the toluene-ammonia mixture is likely still a good solvent for the siloxane

polymers studied here. Each sample was again weighed periodically until equilibrium was reached with the toluene/ammonia mixture (~ 30 days). The samples were then dried overnight under vacuum or under ambient conditions for seven days and reweighed for the final dry weight. The weights were then used in a modified Flory-Higgins approach discussed in detail in ref. 6 to obtain the crosslink densities due to the polymer network, ν_{poly}, the polymer and the filler, ν_{filler}, and the total crosslink density, ν_{total}, where $\nu_i = MW_{monomer}/MW_{i\text{-}crosslinks}$ and $MW_{i\text{-}crosslinks}$ is the molecular weight between crosslinks derived from the Flory-Higgins equation. As mentioned in ref. 6 and 7, the molecular weights between crosslinks are additive (i.e. $MW_{polyl}=MW_{total} + MW_{ffiller}$) and not the crosslink densities.. All the volume fractions calculated were corrected for the volume of the filler, which would not swell. Given the unknown nature of the polymer formulation, including the exact filler content, the crosslink densities should be considered measures of crosslink density relative to each other and not absolute.

All ^{1}H NMR measurements were performed at 400.13 MRad/s on a Bruker Avance 400 spectrometer using a Bruker TBI (HCX) 5mm probe. ^{1}H $\pi/2$ excitation pulses of 6 μs and relaxation delays of 7 seconds were used. In all cases, small (0.1 cm x 0.1 cm x 0.1cm) squares of elastomer were cut from a larger piece and set in the portion of a 5 mm NMR tube that would be within the coil volume of the probe. Spin-echo decay curves were obtained using a standard Hanh echo sequence shown in Figure 1A with delays between pulses ranging from 10 μs to 40 ms. The echo decay curves were normalized to the extrapolated t=0 intensity. These normalized curves were then fit to a bi-exponential decay, including a term for non-exponential decay due to residual dipolar couplings[9]:

$$EI(t) = X_A \exp(-2t/T_{2b} - \langle\Omega_d^2\rangle \tau_s^{\,2}.\exp(t/\tau_s) + t/\tau_s - 1) + X_B \exp(-2t/T_{2b}) \qquad \{1\}$$

where the A terms represent the monomers associated with the crosslinked network structure (with a mean square of the residual dipolar couplings of $\langle\Omega_d^2\rangle$ and motional correlation time τ_s), while the B terms represents the monomers associated with the non-network sol fraction and dangling chain ends

characterized by a negligible residual dipolar coupling. It should be noted that due to the number of competing contributions to the echo decay rate, $<\Omega_d^2>$ can usually only be diagnostic of trends in crosslink density or molecular order and even these trends must be interpreted with care given previous observations that the trends can be field dependent.[29, 30]

Multiple quantum NMR experiments were performed using the refocused multiple quantum excitation and reconversion pulse sequence shown in Figure 1B. This sequence was shown to be a versatile method for exciting MQ coherences in silicone systems.[17,18] The phases of the reconversion sequence were cycled in 90º steps with phase inversion on the observe pulse for coherence selections (the pulse sequence excited all even multiple quantum coherences). CYCLOPS was then added to yield sixteen step phase cycle.[17, 18] As described in Saalwächter, the pulse sequence yields the total sum of the even multiple quantum coherences, significantly dominated by the double quantum coherences, S_{mq} ($S_{2Q} > 5*S_{4Q}$).[17] Pulse lengths of 6 μs were used with delay Δ_1 and Δ_2 equal to 4.83 μs and 6.16 μs respectively, leading to a cycle time, τ_c, of 182 μs and scaling factor, *a*, of 0.611. Repeat experiments with increased values of Δ_1 and Δ_2 showed no discernable differences, indicating that at the delays used, no significant distortions due to high duty cycles were observed.[17] The effective evolution time is then given by $t_e = a*t_c$.

This set of data was then normalized with the use of a reference data set, S_{ref}, obtained by removing the alternating phases on the observe pulse. The reference is the sum of all coherences that have not evolved into even quantum coherences.[17] The reference signal was first modified by subtracting the long time decay component assigned to the sol-fraction of the polymer network, $S^*_{ref}(t_e) = S_{ref}(t_e) - S_{ref\text{-}long}(t_e)$.[17] The normalized multiple quantum integral was obtained by calculating for each effective excitation time, t_e,

$$I_{mq}(t_e) = S_{mq}(t_e)/(S_{mq}(t_e)+ S^*_{ref}(t_e)) \qquad \{2\}$$

The referencing of the MQ data set by the reference data set serves to remove the long term decays caused by slow dynamics and transverse relaxation processes and provides a more convenient data set to analyze. This method can be subject to systematic errors in the deconvolution state, as discussed below. Alternate normalization methods have been described in the literature, most notably, as determined from a density matrix formulism, simply by the intensity after a $\pi/2$ excitation pulse.[13] Normalization using the signal intensity after a single pulse, however, requires a more complex fitting scheme in which the long term decay must also be considered in addition to the initial short term growth. The method described by Schneider, et al, requires then approximately half the acquisition time for a complete data set.[13]

For the normalization method used here, semi-empirical mathematical descriptions of the MQ growth have been developed by Saalwächter.[17] In the case of spins characterized by a dominant residual dipolar coupling, and where the double quantum intensity dominates the higher order terms, the multiple quantum growth curve can then described by

$$I_{mq}(t_e) = A*(1- \exp(-B*(<\Omega_d>/2\pi)^2\, t_e^2) \qquad \{3\}$$

In cases where spins can be described by more than one residual dipolar couplings, as in the case of phase separated network structures with discrete and well separated mean residual dipolar couplings, the multiple quantum growth curves can be described by a summation of growth curves

$$I_{mq}(t_e) = \Sigma\, X_i*(1- \exp(-B*(<\Omega_d>_i/2\pi)^2)\, t_e^2) \qquad \{4\}$$

where Xi is the mole fraction of spins that can be described by $<\Omega_d>_i$. Such multidomain contribution MQ growth curves have been observed in silicone polymers[17], and in thin layers of PDMS spin-coated on silica substrates.[19, 25] The MQ NMR data obtained and analyzed in this report were fit to equations

{2} and {3} using a least-squares multivariable fit (X_1, $<\Omega_d>_1$, and $<\Omega_d>_2$) in Matlab. The fits were performed only upto $I_{mq}(t_e) = 0.45$. The method presented here has been shown to be subject to systematic errors.[17] These include an overestimation of the more strongly coupled spins, an insensitivity to small quantities of spins with very low $<\Omega_d>$, and a underestimation of the absolute couplings by less than 5% - due to neglect of longer range couplings.

The theory governing the effects of anisotropic motion on the dipolar couplings between proton nuclear spins is well established.[9, 14, 17, 35] The dipolar couplings between spins *i* and *j* in the absence of motion, $<\Omega_d>^{(i,j)}_{static}$, is generally given by the following equation[31]:

$$<\Omega_d>^{(i,j)}_{static} = \mu_o \gamma_H^2 h/8\pi r_{ij}^3 \qquad \{5\}$$

where μ_o and γ_H are the permitivtiy of free space and the gyromagnetic ratio for protons and r_{ij} is the internuclear distance. It has been shown the for PDMS polymers, $<\Omega_d>_{static}$ is 8.9 kRad/s.[36] In the case of fast chain motions restricted by topological constraints typical in polymeric melts, the dipolar coupling is attenuated to[9,14,17]:

$$<\Omega_d>^{(i,j)}_{motion} = <\Omega_d>^{(i,j)}_{static} S_b \tfrac{1}{2} <3\cos^2\alpha-1> \qquad \{6\}$$

where α is the angle between the internuclear vector and the polymeric chain segment orientation – averaged over all the fast motions - and S_b is the dynamic order parameter. In the following $<\Omega_d>^{(i,j)}_{motion}$ will take the designation $<\Omega_d>$. In the case of simple Gaussian chain statistics, it has been shown that

$$S_b = 3/5\ r^2/N \qquad \{7\}$$

Where N is the number of segments between topological constraints and r=$\mathbf{R}/\mathbf{R}_0$, the deviation of the chain end-to-end vector **R** from its average value, $\mathbf{R}_0$. Substituting for $<\Omega_d^2>$ and the average crosslink density υ_{total} leads to the general proportionality:

$$<\Omega_d^2> = N^{-2} \quad = \upsilon_{total}^2 \qquad \{4\}$$

Invoking standard assumptions in polymer network theory, it has been shown that the residual dipole coupling is also proportional to square of the shear modulus, G'.[7]

RESULTS AND DISCUSSION: Hanh-echo decay curves for the irradiated DC745 samples are shown in Figure 2 and are characterized by a) bimodal decay; b) non-exponential decay behavior, and c) dose dependent change in decay rate. The bimodal decay is a common observance in ^{1}H NMR relaxation studies of silicone polymers.[4-9] Following these studies, the rapidly decaying component is assigned to the proton spins in the crosslinked network while the slower decaying component is assigned to the non-network, sol-species. The non-exponential decay rate has also been observed previously in silicone elastomers and is a consequence of the anisotropic motions causing incomplete averaging of the dipolar couplings leading to mixed Gaussain (solid like) and exponential (liquid like) decay.[9]

The decay curves in Figure 2 have been fit to equation {1} and the dose dependant mean squared residual dipolar couplings, $<\Omega_d^2>$, are shown in Figure 3 and listed in Table 1 and indicate a steady, but non-linear, increase in $<\Omega_d^2>$ with dose. Extracted residual dipolar couplings have been shown to be closely related to the segmental dynamics, the average crosslink density, and the elastic modulus in a broad range of silicone elastomer systems as discussed in equations {5-8}. Though such methods can be used to track relative changes in these parameters, early studies have shown that these methods tend to over estimate the residual dipolar couplings and thus the dynamic order parameters due to contributions

from motions and couplings over a large range of time and length scales and the influence of diffusion of spins through field gradients resulting from internal microscopic voids and/or the inorganic filler surface.[28] The results of such measurements yield potentially misleading conclusions on network ordering. In addition, in the experiments performed here, no spectroscopic signature or relaxation time was observed which could be correlated to the polymer chains directly interacting with the filler surface.

Multiple quantum methods, on the other hand, have shown to be much more selective to network dynamics in the millisecond timescale and are dominated by the residual dipolar couplings between spins within the six methyl group in each monomer. As a result, MQ-NMR has been shown to be more selective to local network structure and dynamics.[13-20] Typical curves for the various network models are shown in Figure 4. A network behaving as a single network with a single residual dipolar coupling shown in Figure 4A and described by equation {3}. This is the case that would be expected for a monomodal network. Three curves are shown with increasing residual dipolar coupling and show that as the segmental dynamics decrease, raising the residual dipolar coupling, the rate of MQ coherence growth increases. For the case of phase separated domains with well separated network structures, as in the case of network polymer chains and polymer chains strongly interacting with the inorganic filler surface, the multiple quantum growth curve reveals itself as a dual growth curve with dual inflection points, as shown in Figure 4B. In the case of a broad distribution of residual dipolar couplings, due for example to a distribution of chain lengths that would be expected in a random crosslinked polymer, the growth curve is predicted, as shown in ref. 17, to produce a MQ growth curve shown in Figure 4C with a slow long time growth term.

Multiple quantum growth curves for the 5, 50, and 250 kGray radiatively aged samples are shown in Figure 5. The initial growth rate was clearly observed to be dose dependent with higher exposures leading to higher growth rates. Fits of the data using equation {3} were only acceptable for the low dose exposures. As the dose increased, it became increasingly difficult to fit the growth curves

with only one site. As a result, we choose to consider two possibilities for fitting the MQ growth curves: a) a distribution of residual dipolar couplings; and b) a bi-modal distribution of dipolar couplings. As can be seen in Figure 4, a broad distribution of residual dipolar couplings leads to a long excitation term in the 5-10 ms range. This was not observed in the materials studied here. This suggests a narrow distribution of couplings is present. The observations of narrow distributions was also observed in the bimodal networks studied by Saalwätcher.[17] A fit of the MQ growth curves to a bi-modal superposition of a relatively large coupling and a lower coupling using equation {4}, however, did adequately reproduce the experimental data, as can be seen in Figure 5. This indicates that there are two distinct network domains in this material. The domain with lower residual dipolar couplings is likely due to the general network polymer chains. The chains associated with the higher residual dipolar couplings we assign to polymer chains either physically or chemically interacting with the silica filler surface or in a domain with significantly higher crosslink density than the more dominant network chains. It has been shown by both NMR and dielectric relaxation studies that surface adsorbed polymers are generally characterized by a reduction in the segmental dynamics.[11, 19, 37-40] Given the lack of any further information regarding the network structure in these composites and the solvent swelling and DSC data below, it is likely that the high residual dipolar coupling spins reside in chains associated with the silica surface.

Results of the fit to equation {4} for a bimodal distribution of residual dipolar couplings are shown in Figure 6 and are listed in Table 1. At low doses, the NMR results suggest the network is dominated (~89 % of monomers) by low residual dipolar couplings near 700 rad/s. The remaining network monomers are in a domain with significantly higher residual dipolar coupling near 3200 rad/s. As the dose increased, the residual dipolar couplings in each domain increased from ~700 rad/s to ~1100 rad/s and from ~3200 rad/s to ~3900 rad/s while the mol.% in each domain also changed, with the more ordered network equilibrating with the less ordered network (5 kGray, X_{high} = 0.11; X_{low} = 0.89; 250

kGray, X_{high} =0.25; X_{low} = 0.75). Assuming a 30 wt.% filler content with a surface area of ~ 300 m2/g of which 25% are accessible to the polymer, and four monolayers with a thickness of ~ 0.7 nm each,[24] it is estimated that the adsorbed chains would make up ~ 10 wt.%. Previous studies using both ^{29}Si {^{1}H} cross polarization methods and solvent swelling methods (see below) have shown that high doses of radiation can cause covalent bonding of the polymer chains to the inorganic surface.[6, 7, 41, 42] The data obtained here is consistent with a scenario in which radiation causes not only random crosslinking in the polymer network, but also the increasingly thick layer of polymeric chains interacting either directly or indirectly with the inorganic surface.

The NMR studies reported below were then validated with solvent swelling studies and thermal methods. Calculated crosslink densities from equilibrium swelling weights are shown in Figure 7 and show that with increasing dose, the crosslink density increased not only in the overall crosslink density, υ_{total}, but also in the both the contributions due to the polymer network, υ_{poly}, and the filler-polymer interaction, υ_{filler}. In general the solvent swelling data shows that with exposure to γ-radiation in an N_2 atmosphere radiative crosslinking occurred in the polymer network. The increase in the contribution due to the filler-polymer interaction, in particular, indicates that the number of polymer chains influenced by hydrogen bonding to the filler surface increased with exposure to radiation, consistent with our assignment of the high residual coupling chains to surface adsorbed chains. Comparison of the residual dipolar couplings obtained from the spin-echo and MQ studies with the crosslink densities determined from solvent swelling are shown in Figure 8 and show reasonable agreement with the trends predicted by equation {8}. No particular effort was made to fit the data to a quadratic dependence since over this limited change in crosslink densities, the dependence can be treated as roughly linear.

DSC thermograms with and without a 3 hr isothermal soak at -40 ºC of the radiativley aged materials are shown in Figure 9. The thermograms obtained without a isothermal soak were characterized by a glass transition temperature, T_g, at ~ -120 ºC and a melting endotherm in the heating

curve at T_m = -40 ºC. T_g was not observed to be a function of cumulative dose in these samples while both T_m and the heat of fusion, ΔH_m, were observed to decrease with cumulative dose, and increased crosslink density. This observation is consistent with the increased crosslink density seen in the NMR and solvent swelling data. We have previously reported that for a different filled PDMS/PDPS formulation, that the heat of melting depended on cumulative dose exposure to γ-radiation.[8] With increasing dose, the heat of melting steadily decreased because for a given dwell time at low temperatures, a decreasing fraction of chains were able to rearrange for crystallization. As can be seen in Figure 9B, the heat of melting for the irradiated materials steadily decreases with increasing dose. As shown in ref 6 and 8, a portion of this decrease could be recovered if the dwell time at low temperature was increased due to dramatic changes in the crystallization kinetics.[8] Thermograms of samples subject to a 3hr isothermal soak at -40 °C are shown in the lower curve of Figure 9A. No appreciable change in ΔH_m was noted for any of the samples indicating that for the dominant melt peak the kinetics of crystallization are rapid. A new broad melt feature, however, centered at about T_{m2} = -72 ºC was observed in all samples subject to the isothermal soak. This feature likely represents melting of network chains subject to fewer degrees of motional freedom – i.e. sites near locally higher crosslink density or sorbed at the filler interface. In siloxane polymers, a change in T_m of 20 °C would require a difference in crosslink density of ~ 400 %.[8] Deconvolution of the DSC thermogram suggests that these chains may represent as much as 5-10 % of the polymer chains melting. Though DSC is not generally considered quantitative, these numbers are consistent with the values for the high residual dipolar coupling sites observed by the MQ data, above.

The changes observed in the crystallization behavior of the aged DC745 materials are consistent with the changes by NMR and solvent swelling. With increasing exposure to γ-radiation, random crosslinking occurs. The result of this crosslinking is to decrease the motional mobility of the polymer

chains, as seen in the NMR data, and stiffen the polymer matrix. As the crosslink density increased, the ability of the polymer chains to rearrange for crystallization decreased and the heat of fusion for melting steadily decreased, either due to slowing down of the crystallization kinetics, or due to a decrease in the magnitude of the crystalline domains. The increased contribution of the filler-polymer interaction to the overall crosslink density with increased cumulative dose further reduces the ability of the polymer network to reorganize, reducing both the amount (as measured by ΔH_m) and the temperature of the crystallization.

CONCLUSIONS: We have used both Hanh-echo relaxation time measurements and ^{1}H static multiple quantum methods to assess changes in the network structure in a series of radiatively aged PDMS based elastomers based on the Dow Corning DC745 gum stock. The materials are copolymers with a complex silicon oxide filler particles and a crosslinked network. The NMR data suggests that with increasing exposure, DC745 undergoes radiative crosslinking reactions that, up to 25 MR do not increase significantly the sol fraction of the network. The MQ NMR further suggests a bi-modal network with narrow distributions of residual dipolar couplings. Speciation in the two domains is dose dependent. The high residual dipolar coupling has been assigned to surface adsorbed species. The lower residual dipolar coupling spins correspond to methyl groups far from the filler surfaces.

As the polymer is exposed to increasing cumulative doses, we postulate that the following events occur: 1) an increasing number of polymer chains near the surface adsorb to the filler surface, decreasing their molecular mobility; 2) polymer chains within the network and near the interfacial chains crosslink to these interfacial chains, increasing dramatically their residual dipolar coupling; and 3) increasing crosslinking throughout the network chains as the dose increases. The increased percentage of polymer chains associated with the polymer surface would have significant impact on the

time dependent service variables that may be important for such materials, including stress relaxation and the formation of compression set.

The extension of recently reported MQ NMR methods to radiatively damaged filled systems shown in this study further demonstrates the additional insight obtainable from multiple quantum NMR analysis compared to traditional relaxation and lineshape based methods, particularly in systems where detailed characterization of the network structure is unobtainable by other means (GPC, for example).

ACKNOWLEDGEMENTS: This work was performed under the auspices of the U.S. Department of Energy by the Lawrence Livermore National Laboratory under contract # W-7405-ENG-48. The authors would like to thank Mark Wilson (Honeywell) for sample preparation and Jeff DeBisschop (LLNL) for sample irradiations.

FIGURE CAPTIONS

Figure 1. Pulse sequences used in this study, A) Hanh-echo; B) Multiple quantum excitation, reconversion, and observe sequence. Details of pulse phases and delays are discussed in the text.

Figure 2. Hahn-echo decay curves for irradiated elastomers for cumulative doses of 5, 30, 100, and 250 kGray.

Figure 3. Mean square residual dipolar coupling, $<\Omega_d^2>$, of irradiated elastomers from solid-echo decay curves as a function of cumulative dose.

Figure 4. Representative plot of I_{MQ} as a function of MQ mixing time for (A) increasing values of the residual dipolar coupling, $<\Omega_d>$ = 400, 600, and 800 rad/s; (B) Dual morphology model, described by equation {4} with equal populations of sites with $<\Omega_d>_1$ = 400 and $<\Omega_d>_2$ = 1000 rad/s; (C) Distribution of residual dipolar couplings, described in reference {17} centered at 600 rad/s with a Gaussian width of 100 rad/s. {B} and {C} have been vertically offset for clarity.

Figure 5. Experimental MQ growth curves, I_{MQ} vs. mixing time, for irradiated elastomers with cumulative doses of 5, 50, and 250 KGray. Lines are simulated growth curves assuming either single or dual residual dipolar couplings: A: single $<\Omega_d>$ with X_1 = 0.25; B: single $<\Omega_d>$ with X_2 = 0.75; C: sum of A and B; D: best fit of 250 kGray growth curve to a single $<\Omega_d>$.

Figure 6. Results of 3 parameter fits to equation {4} of $I_{MQ}(t)$ curves shown in Figure 7 as a function of cumulative dose. (A) changes in mole fraction, X_1; (B) changes in residual dipolar couplings, $<\Omega_d>_1$ and $<\Omega_d>_2$

Figure 7. (A) Crosslink densities, ν_{poly}, ν_{total}, ν_{filler}, of irradiated elastomers obtained from two phase solvent swelling experiments as a function of cumulative dose; (B) Plot of ν_{poly}, ν_{total}, ν_{filler}, as a function of mean square residual dipolar coupling from spin-echo studies, $<\Omega_d^2>$, for irradiated elastomers.

Figure 8. Plot of crosslink density as a function of residual dipolar couplings from MQ-NMR experiments. Crosslink densities derived from two phase solvent swelling experiments: (A) ν_{poly}, ν_{total}, and ν_{filler} vs $<\Omega_d>_1$ vs; (B) ν_{poly}, ν_{total}, and ν_{filler} vs. $<\Omega_d>_2$.

Figure 9. (A) Melting portion of DSC thermograms for elastomers irradiated to the indicated cumulative dose. Dashed line: no isothermal soak; Solid line: obtained with isothermal soak of 3 hrs at -40 ºC. Curves clearly indicate dose dependent changes in melt temperature and melt heat of fusion. (B) Change in melt temperature, T_m, as a function of cumulative dose for irradiated samples.

TABLES.

TABLE 1. Results of experimental parameters for samples studied. ni values from solvent swelling experiments. X_{long} and $<\Omega_d^2>$ from Hahn Echo experiments. X_1, $<\Omega_d>_1$ and $<\Omega_d>_2$ from MQ experiments.

	$\nu_{polymer}$ {x10^4}	ν_{total} {x10^4}	ν_{filler} {x10^4}	X_{long} (±2)	$<\Omega_d^2>$ (x10^5 rad^2 s^{-2})	X_1	$<\Omega_d>_1$ (rad/s)	$<\Omega_d>_2$ (rad/s)
5 kGray	4.98	10.49	9.50	9.5	2.1	0.89	700	3200
10 kGray	5.27	10.74	10.35	11.5	2.1	0.87	702	3000
30 kGray	6.25	11.77	13.33	10.2	2.3	0.86	717	3095
50 kGray	5.98	13.25	10.90	10.2	2.6	0.85	803	3376
100 kGray	7.52	15.62	14.50	10.0	3.1	0.81	806	3190
250 kGray	11.25	24.12	21.09	11.0	6.0	0.75	1113	3900

REFERENCES

1. Bovey, F. A., *NMR of polymers* Academic San Diego, CA:1996
2. Schmidt-Rohr, K,; Spiess, H. W. *Multidimensional solid-state NMR and polymers* Academic San Diego, CA:1994
3. Ando, I.; Asakura, T. *Solid State NMR of Polymers* Elsevier Science, London 1998
4. Charlesby, A.; Folland, R., *Radiat Phys Chem* **1983**; *15*: 393.
5. Folland, R.; Charlesby, A., *Radiat Phys Chem* **1977**; *10*: 61.
6. Chien, A.; Maxwell, R. S.; Chambers, D.; Balazs, B;, LeMay, J., *J Rad Phys Chem* **2000**; *59(5-6*): 493.
7. Maxwell, R. S.; Balazs, B;, *J Chem Phys* **2002**; 116: 10492. Note, this paper details the study of a different formulation developed by the U. S. DoE than the formulation discussed here.
8. Maxwell, R. S.; Cohenour, R.; Sung, W.; Solyom, D.; Patel, M., *Poly Deg Stab* **2003**; *80(3)*:443.
9. Cohen-Addad, J. P., *Prog NMR Spect* **1993**; *25*:1.
10. Gronski, W.; Hoffmann, U., Simon, G., Wutzler, A., Straube, E. *Rubber Chem. Tech* **1992***; 65* 63.
11. Grinberg, F.; Garbarczyk, M., Kuhn, W. *J Chem Phys* **1999**; *111(24)*:11222.
12. Fechete, R.; Demco, D. E.; Blumich, B., *Macromolecules* **2002** ; *35*: 6083.
13. M. Schneider, M.; Gasper, L., Demco, D. E., Blumich, B., *J Chem Phys* **1999**; *111***,** 402.
14. Dollase, T.; Graf, R.; Heuer, A., Spiess, H. W.;. *Macromolecules*, **2001***; 34***,** 298.
15. Graf, R.; Heuer, A.; Spiess, H. W., *Phys. Rev. Lett*., **1998***; 80* 5738.
16. Graf, R.; Demco, D. E;, Hafner, S.; Spiess, H. W., *Solid State NMR*, **1998**; *12***:** 139.
17. Saalwächter, K.; Ziegler, P.; Spyckerelle, O. ; Haidar, H.; Vidal, A., Sommer, J-U. *J CheM Phys* **2003**; *119 (6)*: 3468-3482.
18. Saalwächter, K., *J Chem Phys* **2004**; *120(1)*:454.
19. Wang, M.; Bertmer, M.; Demco, D. E.; Blumich, B.; Litvinov, V. M.; Barthel, H., *Macromolecules* **2003**; *36*: 4411-4413.
20. Fechete, R. ; Demco, D. E. ; Blumich, B., *J Mag Res* **2004**; *169(1)*:19.

21. Callaghan, P. T.; Samulski, E. T., *Macromolecules*, **1997**; *30(1)*: 113.

22. Callaghan, P. T.; Samulski, E. T., *Macromolecules.* **2000**; *33(10*):3795.

23. Grinberg, F.; Kimmich, R.; Moller, M.; Molenberg, A., *J Chem Phys* **1996**; *105:* 9657.

24. Jagadeesh, B., Demco, D. E., Blumich, B., *Chem. Phys. Let.* **2004**, *393*, 416.

25. Hafner, S., Demco, D. E., Kimmich, R., *Solid State NMR*, **1996**, *6*, 257.

26. Whittaker, A. K., Bremner, T., Zelaya, F. O., *Polymer*, 1995, 36, 2159.

27. Ernst, R. R.. Bodenhausen, G.; Wokaun, A., *Principles of Nuclear Magnetic Resonance in One and Two Dimensions*, New York; Oxford University Press; 1987.

28. Kenny, J. C., McBrierty, V. J., Rigbi, Z., Douglass, D. C. *Macromol.* **1991**, *24*, 436.

29. Luo, H., Kluppel, M., Schneider, H., *Macromol*. **2004**, *37*, 8000

30. Saalwächter, K., *Macromolecules*, 2005, 38, 1508.

31. Flory, P. J., *Principles of Polymer Chemistry*, Cornell University Press, Ithaca, New York (1953).

32. Polmanteer, K.; Lentz, C., *Rubber Chem. Technol*. **1975**, *48*, 795.

33. Vondracek, P., Vallat, M. F., Schultz, J., *J. Adhesion*, 1991, 35, 105

34. French D. *J. Appl. Poly. Sci.*, **1980**; *25*: 665.

35. Mehring, M., *Principles of High Resolution NMR in Solids*, Springer-Verlag, Berlin, 1983.

36. Friedrich, U.; Schnell, I.; Demco, D. E.; Spiess, H. W., *Chem. Phys. Lett.* **1998**, *285*, 49.

37. Lorthioir, C.; Alegria, A.; Colmenero, J.; Deloche, B., *Macromol*. **2004**; *37*: 7808.

38. Hartmann, L.; Kremer, F.; Pouret, P.; Leger, L.; *J. Chem. Phys*. **2003**; *118*: 6052.

39. Kremer, F.; Hartmann, L.; Serghei, A.; Pouret, P.; Leger, L., *Eur. Phys. J E* **2003**; *12*: 139.

40. Lorthioir, C.; Auroy, P.; Deloche, B. ; Gallot, Y., *Eur Phys. J. E.* **2002**; *7*: 261.

41. Bachmann, S. ; Melo, L. F. C.; Silva, R. B.; Anazawa, T. A.; Jardim, I. C. S. F.; Collins, K. E.; Collins, C. H.; Albert, K., *Chem. Mater*. **2001**, *13*, 1874.

42. Aramata, M. ; Igarashi, T., *Bunseki Kagaku*, **1987**, *47*, 971.

Figure 1.

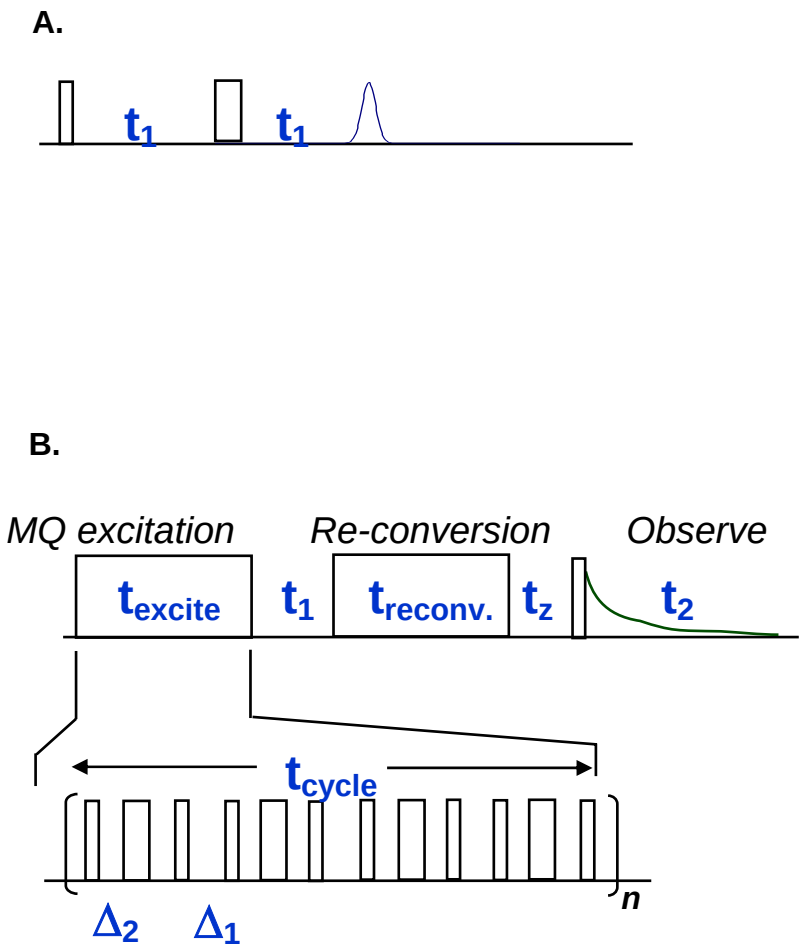
A.
t1
t1
B.
MQ excitation
Re-conversion
Observe
texcite
t1
treconv.
tz
t2
tcycle
n
Δ2
Δ1

Figure 2.

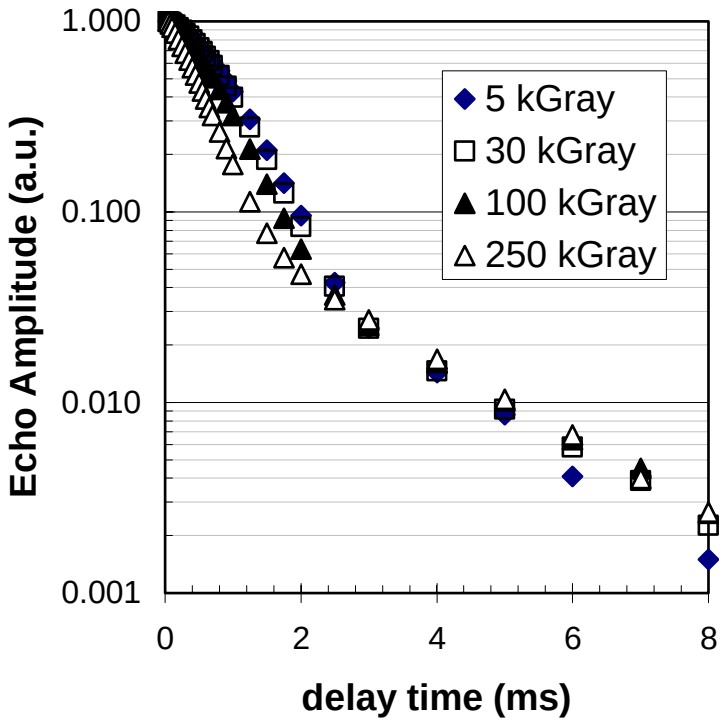
1.000
0.100
0.010
0.001
Echo Amplitude (a.u.)
0
2
4
6
8
delay time (ms)
5 kGray
30 kGray
100 kGray
250 kGray

Figure 3.

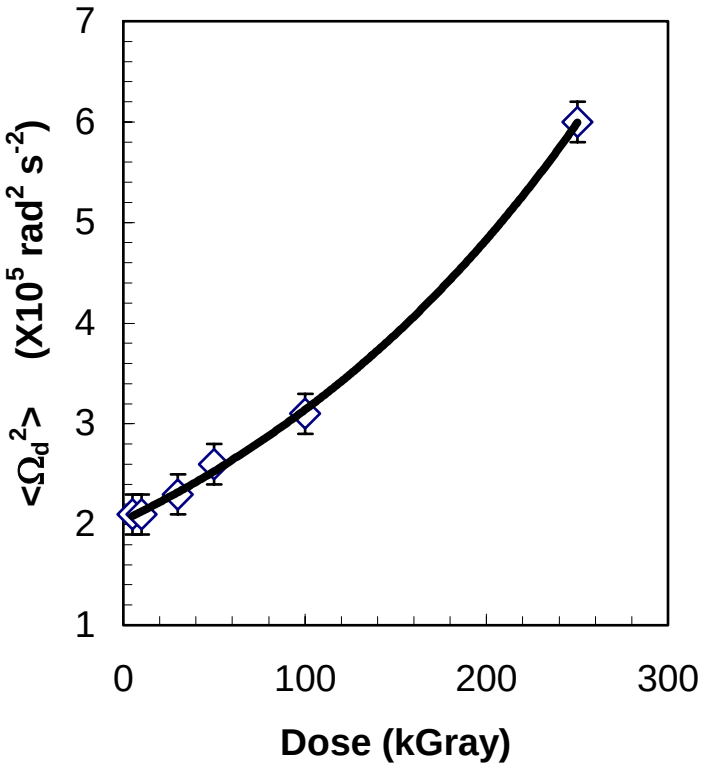

Figure 4.

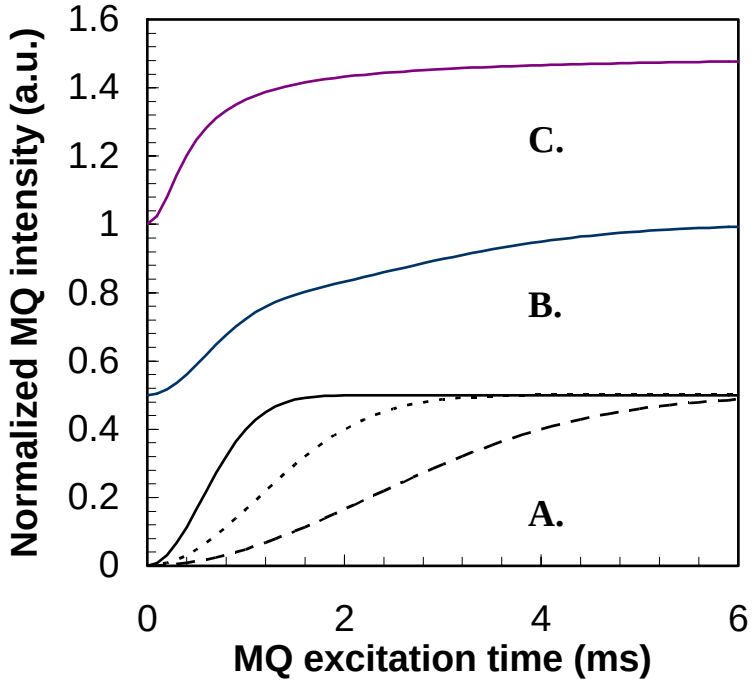
Normalized MQ intensity (a.u.)
1.6
1.4
1.2
1
0.8
0.6
0.4
0.2
0
C.
B.
A.
0
2
4
6
MQ excitation time (ms)

Figure 5.

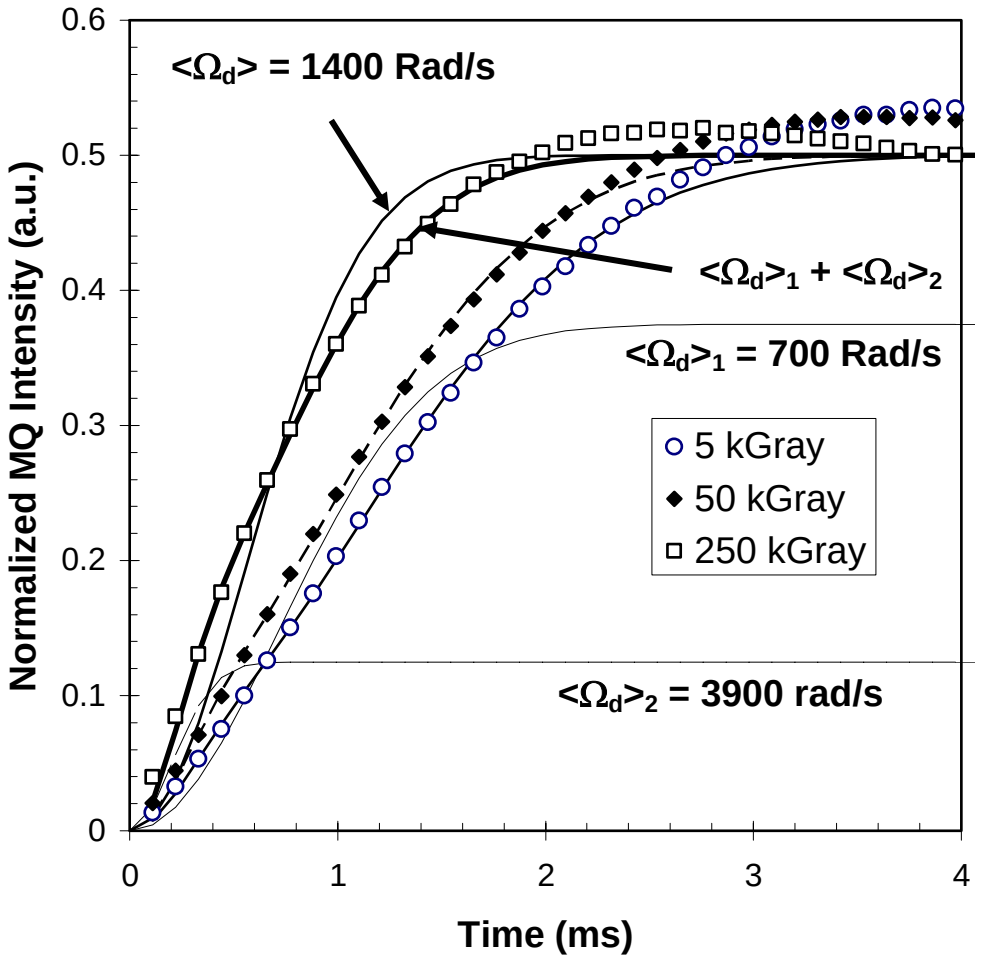
0.6
0.5
0.4
0.3
0.2
0.1
0
0
1
2
3
4
Normalized MQ Intensity (a.u.)
Time (ms)
<Ωd> = 1400 Rad/s
<Ωd>1 + <Ωd>2
<Ωd>1 = 700 Rad/s
<Ωd>2 = 3900 rad/s
5 kGray
50 kGray
250 kGray

Figure 6.

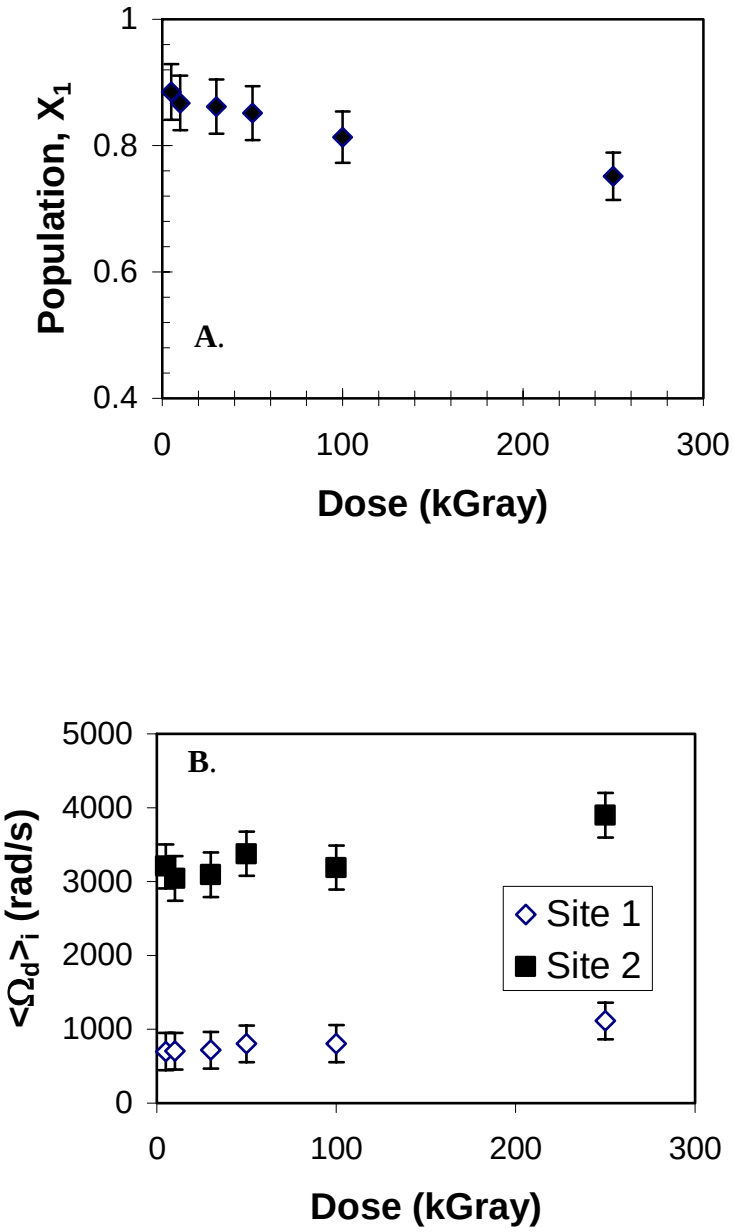
1
0.8
0.6
0.4
Population, X1
A.
0
100
200
300
Dose (kGray)
5000
4000
3000
2000
1000
0
<Ωd>i (rad/s)
B.
Site 1
Site 2
0
100
200
300
Dose (kGray)

Figure 7.

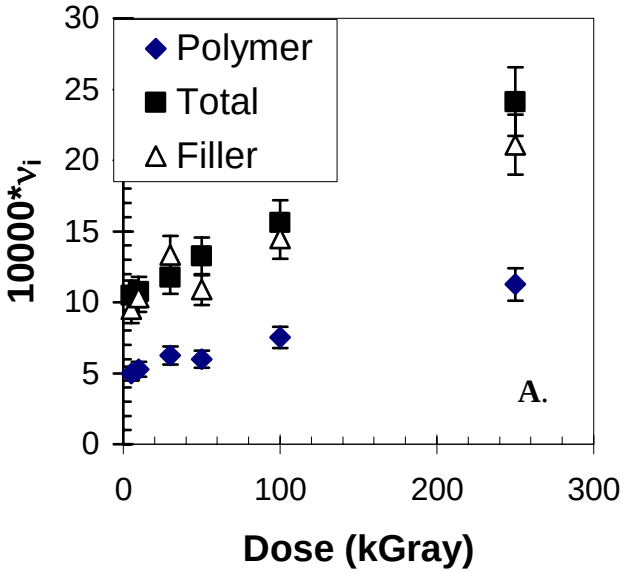
30
25
20
15
10
5
0
0
100
200
300
Polymer
Total
Filler
10000*ν_i
Dose (kGray)
A.

.

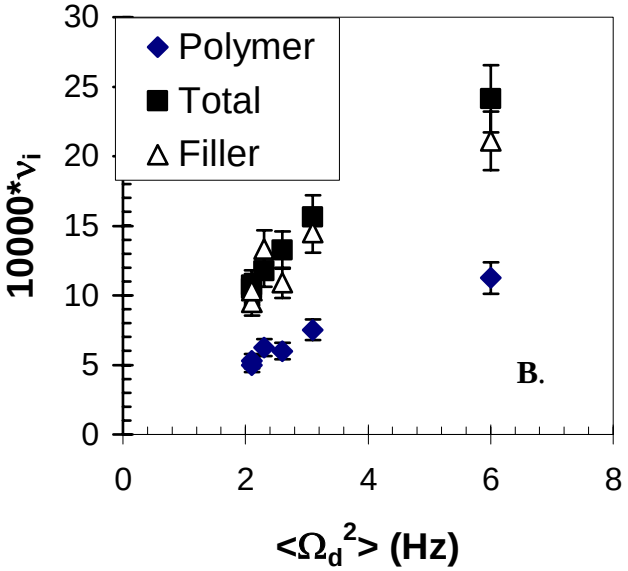
30
25
20
15
10
5
0
0
2
4
6
8
Polymer
Total
Filler
10000*ν_i
$<\Omega_d^2>$ (Hz)
B.

Figure 8

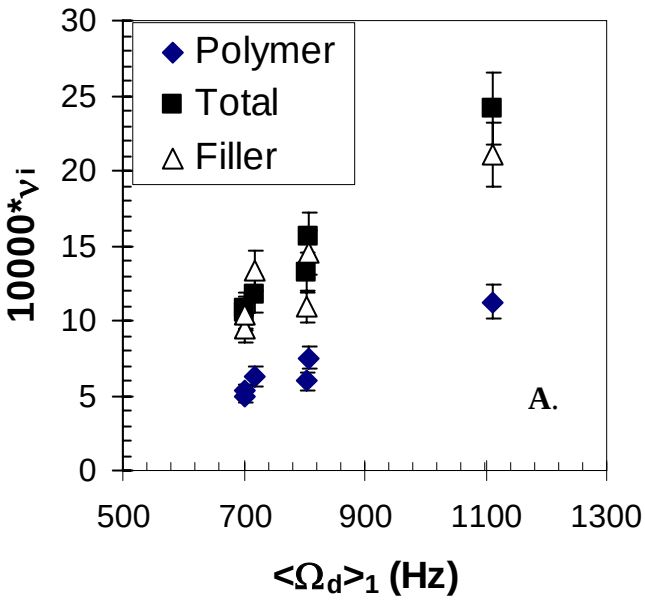
Polymer
Total
Filler
10000*νi
<Ωd>1 (Hz)
A.
0
5
10
15
20
25
30
500
700
900
1100
1300

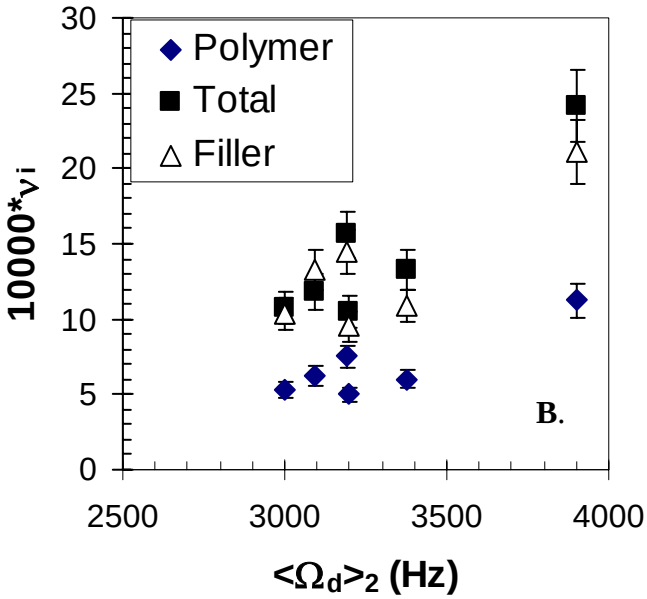
Polymer
Total
Filler
10000*νi
<Ωd>2 (Hz)
B.
0
5
10
15
20
25
30
2500
3000
3500
4000

Figure 9.

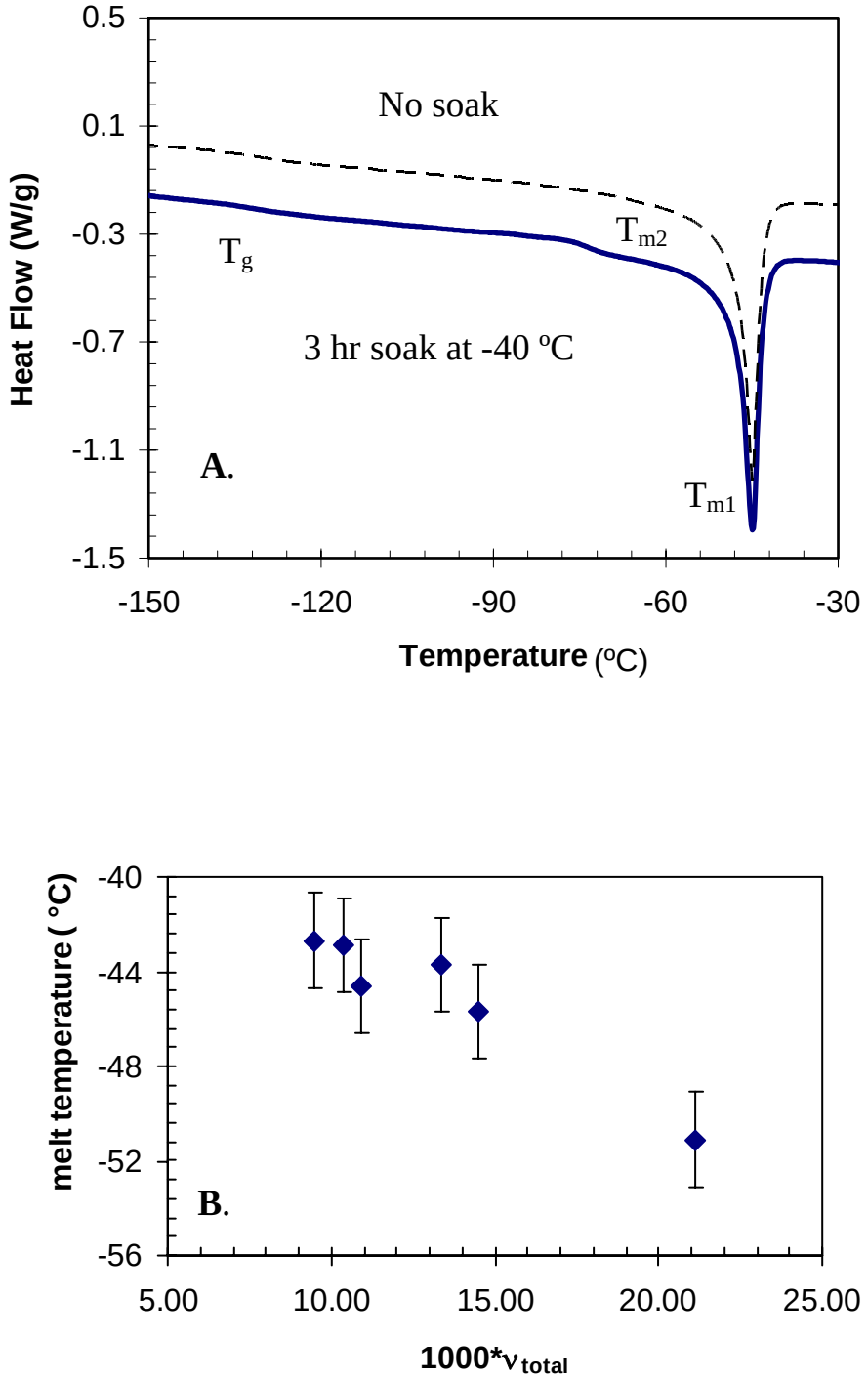
0.5
0.1
-0.3
-0.7
-1.1
-1.5
Heat Flow (W/g)
No soak
T_g
T_{m2}
3 hr soak at -40 ºC
A.
T_{m1}
-150
-120
-90
-60
-30
Temperature (ºC)
-40
-44
-48
-52
-56
melt temperature (°C)
B.
5.00
10.00
15.00
20.00
25.00
1000*ν_{total}